

# From plasmon-enhanced molecular spectroscopy to plasmon-mediated chemical reaction

Chao Zhan, Xue-Jiao Chen, Jun Yi, Jian-Feng Li, De-Yin Wu, Zhong-Qun Tian\*

State Key Laboratory for Physical Chemistry of Solid Surfaces, College of Chemistry and Chemical Engineering, Collaborative Innovation Center of Chemistry for Energy Materials, Xiamen University, Xiamen 361005, China. \*e-mail: [zqtian@xmu.edu.cn](mailto:zqtian@xmu.edu.cn)

## Abstract

The excitation of surface plasmons (SPs), collective oscillation of conduction electrons in nanostructures, can redistribute photon, electron and heat energy in time and space. Making use of this ability, plasmon-enhanced molecular spectroscopies (PEMS) with ultra-high sensitivity and surface selectivity have attracted much attention and developed significantly in the past four decades. Recently, SPs have impacted the discipline of chemistry, through plasmon-mediated chemical reactions (PMCR). PMCR exhibit some obvious differences from, and potential advantages over traditional thermal-chemistry, photo-chemistry and photo-catalysis. Our physicochemical understanding of PMCR is still far from complete. In this review, we analyze the common ground and distinctive features of PEMS and PMCR; comparing as well, PMCR and traditional photo-chemical and thermal-chemical reactions. We then discuss how to advance PMCR by rationally designing and fabricating plasmonic nanostructures, selecting suitable surface/interface mediators and teaming them synergistically.

## Introduction

Surface plasmons (SPs) play a critical role in the optical properties of nanostructured metals (Au, Ag, Cu, etc.) and heavily-doped semiconductors. They can even be used to reduce the commonly-encountered optical diffraction limit by concentrating electromagnetic radiation into spaces with subwavelength dimensions, enabling large local field enhancements in the vicinity of nanostructures sustaining localized surface plasmons (LSPs).<sup>1,2</sup> The field studying the fundamentals and applications of nanostructure-based SPs is known as nanoplasmonics, which has expanded in the past decade or so from plasmon physics (including plasmon-enhanced molecular spectroscopy, sensing, plasmon heating, wave guiding, etc.) to embrace plasmon-mediated chemical reactions (PMCR) as well as plasmon induced chemical phenomena generally.<sup>3-19</sup>

The interface between these two applications of plasmons is not sharp, plasmon physics, includes PEMS (plasmon-enhanced Raman, IR and fluorescence spectroscopies, etc.) that have been studied since the mid-1970s.<sup>3,4</sup> In 1981 the idea of using SPs to enhance chemical reactions was first proposed then experimentally realized two years later.<sup>20,21</sup> At present, over four thousand publications appear

annually on PEMS; while several hundred papers are published annually on PMCR, as a reflection of the relative youth and greater complexity of the latter. The mechanisms of PEMS have been widely investigated, especially in the context of plasmon-enhanced Raman spectroscopy (PERS). By contrast our physicochemical understanding of PMCR is still far from complete. One of the themes we will review in this article is the extent to which what has been learned regarding PEMS over the past four decades may enlighten our understanding and development of PMCR. In its earliest incarnations PMCR was often studied using PERS; for example, an enhanced or accelerated photochemical process might have been tracked using the time evolution of the SERS spectra of the reaction products, excited by the same laser that induced the (enhanced) photochemistry.<sup>22</sup> In such experiments the nanostructure-based plasmonic enhancement was exploited in two ways: enabling a strong photochemical response, and allowing the time-dependent concentration of the products, often produced in meager quantities, to be reliably measured.<sup>23-26</sup>

Nevertheless, intimately related PEMS and PMCR also differ in crucial ways. Usually, there are more challenges in PMCR compared with PEMS because of the molecular transformation involved. For example, PEMS measurements obtain the better detection sensitivity when probed molecules bond to the plasmonic metal surface, while the over-strong bonding/adsorption causes problems for PMCR, like the blocking of active sites for chemical reactions.<sup>27,28</sup> Verifying which reaction SPs can mediate is not enough, the more important tasks are to fully understand the uniqueness of PMCR and to explore how efficiently advance the plasmonic powered chemical process.

The growth and future of PMCR critically depend on the fundamental understanding of SPs properties and how they enable chemical reactions. In the first section, we discuss the basics of SPs, PEMS and PMCR, and how these processes function under varying conditions from the plasmonic nanostructure only to the plasmonic nanostructure interacting with the molecule/material with and without chemical reactions. Here, because most of the current work on PMCR was carried out on nanostructures, we pay more attention to LSPs. For the basics of PEMS, primary contents are focused on PERS considering its pivotal role in the PEMS history and the significant contributions to the PMCR study. Also, we try to describe the scientific intent and advantage of PMCR when compared to thermal chemistry, photochemistry and photocatalysis. Next, we discuss various factors which significantly affect PMCR, followed by the correlation of PEMS and PMCR. In the last section we discuss possible strategies for improving reaction efficiency, selectivity and other opportunities with PMCR. Throughout, we attempt to clarify the special characteristics of PMCR by comparing and contrasting it to PEMS and to other reaction systems, hopefully resulting in a relatively complete current description of PMCR.

## **Nanostructure-based surface plasmons (SPs)**

### **The excitation of SPs**

Most plasmonic substrates are based on the coinage metals (Au, Ag or Cu) because such metallic nanostructures can support intense SPs, collective oscillating

modes of the conduction electrons at metal/dielectric interfaces, with resonances in or near the visible portion of the spectrum. The emphasis on that wavelength range arises from two priorities, the first is the availability of laser and lamp-based light sources in that wavelength range; the second is the tacit goal of being ultimately able to develop photochemical techniques that might be powered by sunlight. SPs are normally divided into two categories: (i) localized surface plasmons (LSPs, as shown in Figure 2), in which electrons coherently oscillate locally within and in the vicinity of a nanostructure and (ii) propagating SPs, surface plasmon polaritons (SPPs), in which the coherent electron oscillation propagates as a longitudinal wave along the metal surface. When SPs are resonantly excited, the plasmonic structures can concentrate the incident light into a spatially narrow region around the nanostructure, which results in electromagnetic near-field enhancement (Figure 1). The plasmonic structure collects photons over a region larger than its physical size (as an antenna does) concentrating that energy in a much smaller volume.<sup>29,30</sup>

To understand the near-field enhancement qualitatively, a Drude model of a homogeneous metal nanosphere with radius ( $r$ ) much smaller than the incident light wavelength is considered within the electrostatic approximation.<sup>31</sup> As a consequence of the collective oscillation of the conduction electrons, the SPs excitation induces a periodic dipole in the metallic nanostructure, as follows  $\mathbf{p}_{dip} = \epsilon_m \alpha_M \mathbf{E}_0$ . Here, the induced dipolar  $\mathbf{p}_{dip}$  simultaneously depends on the relative dielectric constant of the surrounding medium ( $\epsilon_m$ ), the polarizability of the metal sphere ( $\alpha_M$ ), and the amplitude of the uniformly incident electromagnetic field ( $\mathbf{E}_0$ ). The  $\mathbf{p}_{dip}$  approaches resonance when  $\alpha_M$ , being proportional to  $[\epsilon_M(\omega) - \epsilon_m]/[\epsilon_M(\omega) + 2\epsilon_m]$ , maximizes at  $\epsilon_M(\omega) + 2\epsilon_m$  tending to 0, where  $\epsilon_M(\omega)$  is a frequency-dependent complex dielectric function of the metal sphere. The resonant frequency  $\omega_{LSPR}$  can be obtained directly from the foregoing as  $\omega_{LSPR} = \omega_p/(1 + 2\epsilon_m)^{1/2}$ , in which  $\omega_p$  is the plasma frequency of the bulk metal.<sup>31</sup> Likewise, the strength of the near-/local electromagnetic field  $\mathbf{E}_{loc}$  which is in proportion with  $\mathbf{p}_{dip}$  can be resonantly enhanced at  $\omega_{LSPR}$ . For the coinage metals, the resonance condition is satisfied under visible light excitation, and the  $\text{Im}[\epsilon_M(\omega)]$  is small at the resonance frequency, resulting in their wide application in PEMS and PMCR. Figure 1 shows a picture of plasmon physics, in which the local field distribution and the extinction spectra of some typical Au nanostructures in the absence of molecule are presented. The electromagnetic field near the metal surface is redistributed at the nanoscale (Figure 1b & c), while at some locations, especially in the nanogap of a dimeric structure (Figure 1f), the local electromagnetic field strength can be significantly and controllably enhanced. Furthermore, when the plasmonic nanostructures touch or are close to other materials (Figure 1d & e), the electromagnetic field at the thus-formed interface can also be greatly enhanced, an essential characteristic for the wide application of PEMS and PMCR.

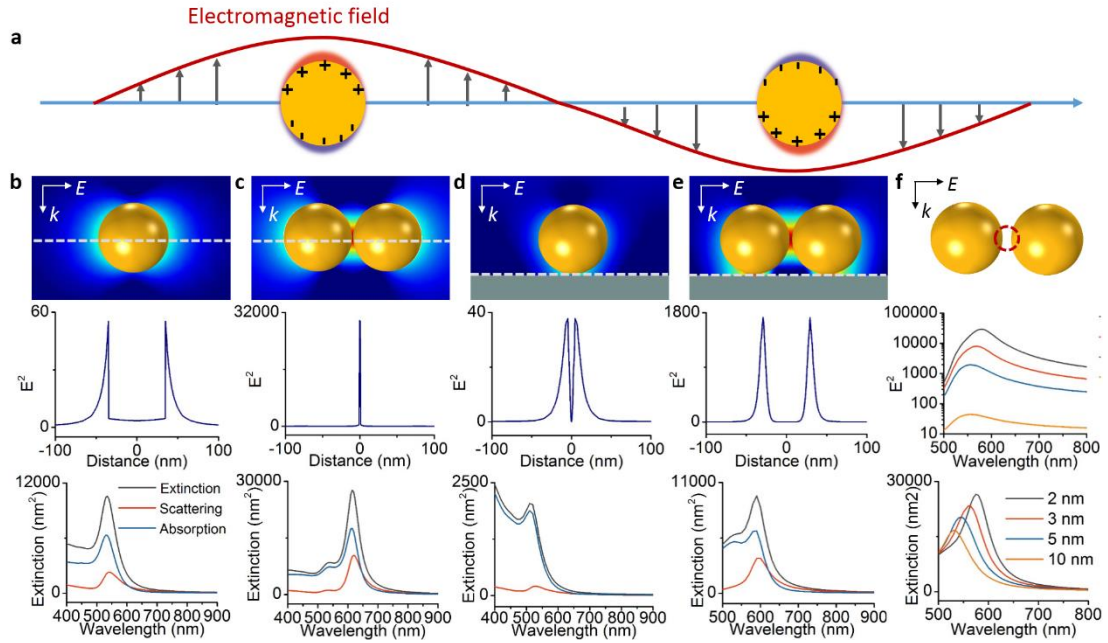


Figure 1. The classical description of SPs excitation, the optical confinement and spectral feature for some typical nanostructures. a, Collective oscillation of conduction electrons in a nanostructure induced by incident light. b-e, Electromagnetic field distributions ( $E^2$ ), and extinction spectra of some typical Au nanostructures computed using finite-element simulations. b, an isolated Au nanosphere with a diameter of 60 nm in vacuum. c, a nanosphere dimer with a gap size of 2 nm in vacuum. d, a single Au nanosphere on a flat Si surface. e, the Au nanosphere dimer with a gap size of 2 nm on Si surface. The particle-substrate gap in (d) and (e) is 1 nm,  $\mathbf{E}$  is the electromagnetic field,  $\mathbf{k}$  is the wave vector of incident light. f, The local field enhancement at the mid-point of the nanogap of Au nanosphere dimer with varied gap sizes from 2 nm to 10 nm.

### The relaxation of SPs

To easily understand the excitation and relaxation of SPs in time sequence, we use a single nanosphere as the model for the following discussion (Figure 2). Thereafter the excitation, the excited SPs in the nanostructure can be relaxed via the re-emission of a photon or the non-radiative paths.<sup>32</sup> The branching ratio between these two decay mechanisms is determined by the radiance of the plasmon mode.<sup>33</sup> The main relaxation process can be separated into several components occurring on different time scales.<sup>34-39</sup> In the first 1–100 fs, the SPs dephase and excited electron-hole pairs are produced by Landau damping and other photon-electron interactions. The thus-formed excited electrons are endowed with energies ranging from the Fermi level  $E_f$  to  $E_f + \hbar\omega_0$ , and the corresponding holes have energies from  $E_f - \hbar\omega_0$  to  $E_f$  ( $\omega_0$  refers to the incident light frequency).<sup>35</sup> During this very short period, the electron-hole pairs with highly non-thermal distribution decay either through the re-emission of photons or the multiplication of carriers via electron-electron interactions. That is, the photonic energy is converted into electronic energy in this process. Thereafter on

a timescale from 100 fs to several ps, the excited carriers interact through electron-electron interactions with lower-energy electrons redistributing their energy into a quasi Fermi-Dirac distribution, as shown in Figure 2b. Finally, the electron-hole pairs relax to thermal energy through electron-phonon, phonon-phonon interactions on a relatively long timescale up to hundreds of picoseconds (Figure 2c). Accordingly, during the excitation and relaxation process of SPs, the energy and spatial redistribution of the photons, electrons and phonons are achieved on different time-scales. The effects induced by SPs can be profitably separated under the following three topics: the electromagnetic near-field, the excited carriers, and the local heating. These effects differ in time, space and energy scales, however, they are all closely related to PEMS and PMCR.

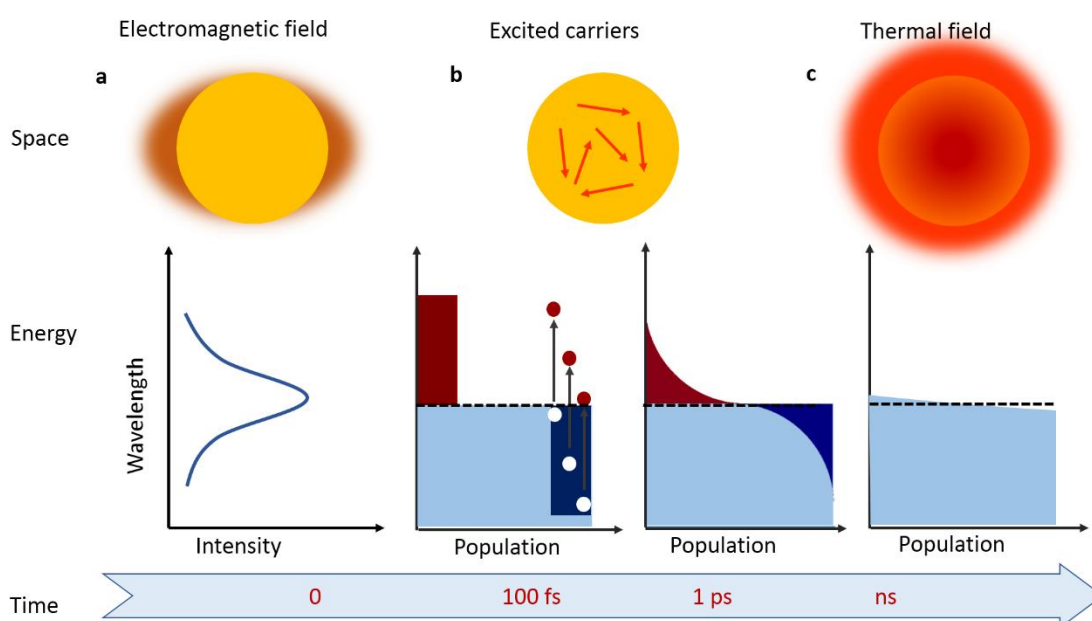


Figure 2. Three main effects induced by the excitation and relaxation of SPs including electromagnetic field enhancement, excited carriers and thermal effect. The schematic diagrams show their characteristics in space, energy and time. a, The redirection of incident light by the excitation of SPs leads to the electromagnetic near-field enhancement, characterized by a specific resonance wavelength for a specific nanostructure. b, The formation and relaxation of the excited carriers. The population of the electronic states is accompanied with the energy conversion from photon to electron, following by the energy redistribution of excited carriers in different time scales. c, Finally the electronic energy converts into thermal energy which leads to the local heating.

### Basics of plasmon-enhanced molecular spectroscopy (PEMS)

We will now consider molecules coupled to plasmonic nanostructures but without chemical reactions, as shown in the top left of Figure 3. PEMS refers to all spectroscopic techniques involving SPs excited by light, including linear and nonlinear processes of molecular absorption, scattering and emission, which leads to a large

family of techniques including plasmon-enhanced infrared spectroscopy (PEIRS),<sup>40-42</sup> plasmon-enhanced Raman spectroscopy (PERS),<sup>11,43-47</sup> plasmon-enhanced fluorescence spectroscopy (PEF),<sup>12,13,48</sup> etc. The enhancement factors of the above spectroscopies are approximately ca.  $|E_{loc}|^2$ ,<sup>49</sup>  $|E_{loc}|^4$ ,<sup>50</sup> and  $|E_{loc}|^2\eta$  (where  $\eta \leq 1$  refers to the emission efficiency),<sup>51</sup> respectively. Because PERS has been the most in-depth studied and applied spectroscopic technique in the PEMS family, we use it to elucidate how plasmonic nanostructures interact with light and molecules for a fundamental understanding of PEMS and to seek the connection with PMCR. For historical development,<sup>52</sup> landmark methods,<sup>46,47,53</sup> and the applications of PERS,<sup>22,47,54,55</sup> we refer readers to the reviews and book chapters cited in this sentence.

### Electromagnetic Enhancement

Raman scattering provides fingerprint vibrational information with high spectral resolution (ca.  $1 \text{ cm}^{-1}$ ) over a wide spectral window ( $5\text{-}4000 \text{ cm}^{-1}$ ). However, the Raman scattering (Figure 3a) cross-section is normally small, typically  $10^6$  and  $10^{14}$  times smaller than that of infrared and fluorescence, respectively.<sup>52</sup> By using plasmonic nanostructures, PERS increases the effective Raman cross-section allowing even the Raman spectra of single molecules to be detected.<sup>56-59</sup> This is primarily due to the enhancement of the electromagnetic near-field in the vicinity of the nanostructure as a consequence of SP excitation (Figure 2a). This process is often referred to as the electromagnetic (EM) SERS enhancement mechanism.<sup>5,8,60-62</sup>

When a probe molecule is in close proximity to the plasmonic nanostructure (top left in Figure 3a), the induced Raman dipole at a given Raman scattered frequency is proportional to the local field strength  $|E_{loc}|$ . In comparison with the normal Raman, the dipolar energy of PERS is enhanced by a factor  $|E_{loc}|^2/|E_0|^2$ . Noting that Raman scattering is a continuous two-step process, i.e. the incident photon ( $\omega_0$ ) interacting with the molecule from the far-field to the near-field and the scattered photon ( $\omega_R$ ) instantaneously emitting from the near-field to the far-field, the EM enhancement factor can be approximately expressed as  $G \approx (|E_{loc}(\omega_0)|^2 / |E_0(\omega_0)|^2)(|E_{loc}(\omega_R)|^2 / |E_0(\omega_R)|^2)$ . An additional approximation is often made for low frequency vibrations when  $\omega_R$  is not very different from  $\omega_0$ , resulting in the familiar  $G \approx |E_{loc}(\omega_0)|^4 / |E_0(\omega_0)|^4$  SERS enhancement expression, the so-called  $|E|^4$  – approximation.<sup>55</sup>

There are two remarkable features of the EM enhancement factor, one is the surface-specificity and the other is the geometry-inhomogeneity. The surface-specificity results from the distance-dependence of  $|E_{loc}|$  which is proportional to  $D^{-3}$  (here,  $D$  is the distance of the probe molecule from the SPs dipole center).<sup>31</sup> Accordingly, from the  $|E|^4$  approximation one can infer that  $G$  is proportional to  $D^{-12}$ , and can thus probe molecules in close proximity to the plasmonic surface whose Raman cross-sections can be greatly enhanced, while molecules residing in the surrounding media are not greatly enhanced (top right in Figure 3a). The geometry-inhomogeneity is a consequence of the spatial localization of the enhanced electromagnetic near-field,<sup>51</sup> determined by the structure and morphology of the plasmonic nanostructure as well as the polarization of the incident light. Usually, EM enhancement factors are higher at the sharp curvature edges, tips and nano-interspaces between coupled particles. The highly localized regions on PERS-active

surface with extraordinarily large enhancement factors are the so-called "hotspots", which contributes most of PERS signals.<sup>51,55</sup> However, the probability of hotspots is much lower than that of the medium- or non-enhanced regions.

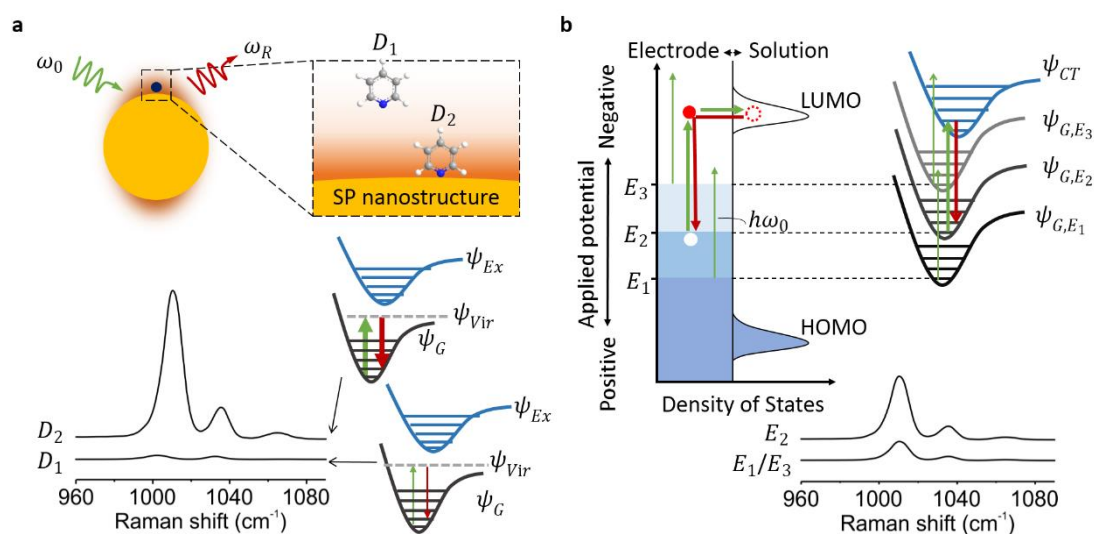


Figure 3. Mechanistic illustration of the plasmon-enhanced Raman scattering (PERS) process and the charge transfer (CT) process. a, The enhancement predominantly derives from the enhancement of electromagnetic local field experienced by the probe molecule near the plasmonic nanostructure, i.e. the EM enhancement. The plasmonic nanostructure serves as the receiving optical antenna that transfers the far field to the near field at  $\omega_0$  and as the transmitting optical antenna that transfers the near field to the far field at  $\omega_R$  (top). The intensity of vibrational bands is proportional to the fourth power of the local field strength ( $|\mathbf{E}_{loc}|^4$ ) which is inversely proportional to the third power of the distance from the plasmonic nanostructure ( $D^{-3}$ ). In total, the intensity of PERS bands is determined by the probability of the Raman scattering transition, the larger the local field strength and the closer the probe molecule to the plasmonic nanostructure, the higher the probability of Raman scattering (bottom). b, CT could be present if the probe molecule interacts strongly with the plasmonic substrate and its energy level and the Fermi level of the metal are appropriate in resonance with the exciting light. A resonant-like Raman scattering process through photon-induced CT is illustrated at the electrode-solution interface where the Fermi level of plasmonic substrate can be easily tuned by the electrode potential to bring about resonance with the incident photon energy  $\hbar\omega_0$  (left). The corresponding probability of the energy state transition and PERS intensity-potential profile maximize when applying at the resonant potential  $E_2$ , and decrease at the off-resonant potentials  $E_1$  and  $E_3$  (right).  $\psi_{Ex}$ ,  $\psi_{Vir}$ , and  $\psi_G$  in a denote the energy state of the first excited state, the virtual state, and the ground state of the probe molecule, respectively, where  $\psi_{G,E_i}$  and  $\psi_{CT}$  in b denote the potential-dependent ground state and the potential-independent CT state of the surface complex, respectively, where the surface complex is the combination of the electrode outmost layer and the adsorbed probe molecule. HOMO and LUMO are the highest occupied molecular orbital and the lowest unoccupied molecular orbital of the

adsorbed molecule, respectively. The thickness of the arrow represents the probability.

### **Chemical Enhancement**

When the probed molecule interacts strongly with the plasmonic nanostructure, the subject to be studied may cross the border from surface physics to surface chemistry. The latter is more complicated which involves surface binding, chemisorption and/or surface complexes of molecules. As a consequence, the enhancement mechanism is generally called as the chemical enhancement (CE) or charge-transfer (CT).<sup>6,50,63</sup> It is well known that the total enhancement of the spectroscopic signal primarily results from SPs, though other non-EM effects including CE/CT contribute to the total enhancement, and their contributions vary from molecule to molecule, accounting for many interesting phenomena.

CT can occur either directly from the molecule to the plasmonic nanostructure or vice versa, or indirectly through surface species such as co-adsorbates, solvent molecules or electrolyte ions. It is therefore necessary to consider three types of charge transfer processes.<sup>64</sup> Type I is a result of a charge transfer between the probe molecule and the surface. It changes the electronic state population and thus the polarizability of the probe molecule, leading to increase or decrease of the Raman scattering signal. Type II involves strong charge-transfer mainly related to the formation of surface complex of the partially charged metal surface atom, the probed molecule and/or the co-adsorbed surface species. Moreover, some surface complexes can be considered as the new molecules that have new electronic transitions in resonance with the incident light, resulting in a resonant Raman process. Type III is photon-induced charge transfer process,<sup>64,65</sup> as observed in some electrochemical Raman spectroscopic experiments (Figure 3b). The change of the applied potential can continuously tune the Fermi level of the plasmonic nanostructure by an external potential. When the incident photon energy matches the energy difference between the adsorbed molecules' orbitals and the metal Fermi level, or between the charge transfer state which was assumed to be potential-independent and the potential-dependent ground state of the surface complex (top right in Figure 3b), they can lead to a resonance-like Raman scattering process in which the amplified Raman intensity reaches a maximum at  $E_2$  (bottom in Figure 3b). As the incident light frequency ( $\omega_0$ ) varies, different applied potentials are needed to ensure resonance with the charge transfer states.

In general, the enhancement either through the EM or CT mechanism can be explained by the increased probability of the Raman scattering process as illustrated in Figure 3. For the former, the probability of electron transition between the electronic ground state and the virtual state increases as a result of the enhanced EM field around the plasmonic nanostructure. While for the latter (types II and III), the probability increases due to the different resonance-like transitions between the electronic real states. Accordingly, the spatial aspect is distinctively different for these two mechanisms, i.e., the EM mechanism is a long-range (about 10 nm) effect while the CT mechanism is a short-range (about 1 nm or less) effect.

It is necessary to emphasize that the CT enhancement is molecule-specific and



dependent on the three entities (molecule, incident photon and plasmonic nanostructure) interaction. The unique characteristic of SPs leads to the unique feature of CT. Because all the CT processes take place under SPs condition (Figure 2), they depend on the strength of the electromagnetic and thermal fields and the density of the excited carriers. More precisely, they should be called SPs-based CT processes. Moreover, the CT and EM can interact with, and influence each other, so that CT especially for the types II and III is improved by EM enhancement, while the CT can change the SPs properties that determine the EM strength.<sup>66</sup> For a comprehensive understanding of PEMS and PMCR and their relationship, great attention needs to be paid to these important and correlated phenomena. It is clear that the SPs-based CT process overlaps PMCR to some extent, in the former case, when probing a molecule, or, in the latter case, when a molecule is undergoing a chemical reaction.

### Basics of plasmon-mediated chemical reactions (PMCR)

According to the basic process of SPs excitation and relaxation (Figure 2), we try to compare the PMCR with three types of relevant reaction systems and establish a new and integrated description for PMCR from the perspective of time, space, energy and probability (Figure 4). It is important to note that these types of SPs effects usually occur together to various extents, and the excitation and relaxation properties of SPs can be influenced by contact with molecules. Based on the careful comparison, we will elaborate the specific characteristics and scientific intension of PMCR which differentiate itself from those well-known reaction systems in the following contents.

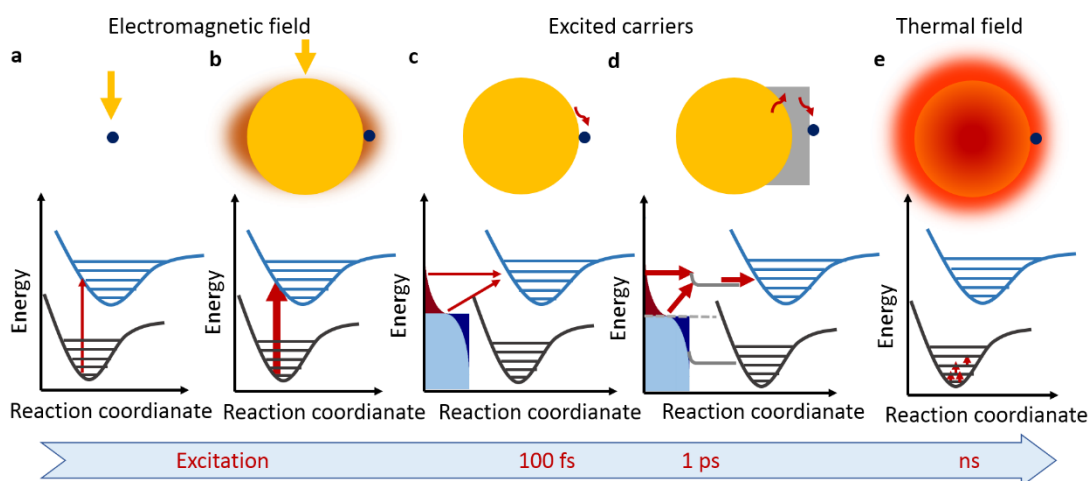


Figure 4. A microscopic view of the plasmon-mediated chemical reactions (PMCR) as it proceeds via various mechanisms. a, A normal photochemical reaction of a molecule initiated by an electronic excitation from the ground state to an excited state to overcome the activation energy. b, Electromagnetic near-field enhancement resulting from SPs greatly increases the probability of molecular excitation for a molecule near the plasmonic nanostructure. This will increase the rate and/or the yield of the photochemical reaction but requires overlap of the absorption spectrum of the plasmonic nanostructure with that of the molecule. In addition, the precursor should be located in the enhanced electromagnetic field. c, SPs excited carriers can transfer

to the molecular near the surface through direct or indirect charge transfer process,<sup>18,67</sup> then mediate the chemical reaction similar as photocatalysis. In this mechanism, the spectrum of plasmonic nanostructure and molecule need not overlap, but the energy of the excited carriers and the electronic band structure of molecules need to match appropriately. Bearing the ultra-short lifetime of those SP-excited carriers in mind, the probability of such photocatalysis-like process is usually low. (However, noting that the lifetimes of SPs excited carriers are very short, the probability of such photocatalysis-like process could be low.) Accordingly, for more efficient charge transfer, the precursor should adsorb on the surface of the plasmonic structure. d, Combined with some mediators such as the semiconductors, the efficiency of PMCR based on SPs excited carriers could be significantly improved. Such heterogeneous structures can increase the probability of charge transfer, and the lifetimes of the carriers transferred to the mediator will be extended which increasing the reaction probability. e, Increased temperature is commonly used to accelerate chemical reactions. Local temperature increases following SPs decay can increase the population of reactants in vibrationally excited states. SP decay also produces temperature increases that are highly localized at the surface where the chemical reaction occurs, a more efficient process than heating the whole reaction chamber. The width of the arrow represents the probability.

#### **Electromagnetic near-field mediated photochemical reaction**

As in traditional photochemistry, electromagnetic near-field mediated photochemistry is associated with electronic excitation of the reactant molecules (Figure 4a, 4b).<sup>68-73</sup> The enhanced electromagnetic near-field enables three effects. (1) A dramatic increase in light absorption due to increased light intensity, and/or the extension of the light path thereby increasing the excitation probability of the reactant or material (Figure 5a1).<sup>74</sup> For example, a 66-fold increase in photocurrent was observed during water splitting under visible light illumination, whereas a 4-fold reduction was seen under ultraviolet light when N-doped TiO<sub>2</sub> (which absorbs visible light) was combined with Au nanoparticles.<sup>75</sup> The enhanced electromagnetic near-field accounted for the photocurrent increase. In a similar system in which an Ag nanostructure was incorporated into a N-TiO<sub>2</sub> photoanode, the increase of the photocurrent was attributed to the enhancement of the electromagnetic field at the interface, and corroborated by the dependence of the photocurrent on light-intensity.<sup>76</sup> (2) Control of photochemical reactions in very small volumes, even on the scale of nanometers. For example, the two-photon polymerization of SU8 was investigated on a nanoblock pattern with 6 nm wide nanogaps (Figure 5a2). By changing the polarization of the light, the reaction proceeded at different positions of the nanoblock substrate which were in agreement with the predictions of a FDTD simulation of the near-field strength.<sup>77</sup> Moreover, non-linear photo-excitation was achieved in this experiment even under low-intensity illumination, another important effect of the enhanced electromagnetic near-field (3). However, overlap of the absorption spectra both of the plasmonic nanostructure and the reaction precursor is essential in order to carry out such a reaction efficiently.

### **Excited carrier mediated photocatalytic reaction**

PMCR carried out by excited carriers, with results comparable to those of photocatalytic reactions in which excited carriers are used to induce chemical reactions (Figure 4c, 4d),<sup>78-82</sup> has been discussed in several excellent reviews,<sup>16,18,39</sup> which conclude that excited electrons (or holes) induced by SPs can be injected from the plasmonic metal either to a neighboring molecule or into a semiconductor possessing suitable energy levels (ranging from  $E_f$  to  $E_f + \hbar\omega_0$  for excited electrons and from  $E_f - \hbar\omega_0$  to  $E_f$  for excited holes) in contact with the plasmonic metal.<sup>83</sup> For example, the photocurrent of water oxidation was reported to be enhanced under visible light upon loading Au or Ag nanoparticles in TiO<sub>2</sub> sol gel films (Figure 4d).<sup>84</sup> In another study, overall water splitting was carried out by the SPs excited electron-hole pairs from nanorod arrays which were in contact with a TiO<sub>2</sub> film under visible light (Figure 5b1).<sup>14</sup> Additionally, a number of other chemical reactions have been induced or enhanced under mild conditions by SP-excited carriers, including catalytic oxidation reactions,<sup>15</sup> H<sub>2</sub> dissociation,<sup>85</sup> N<sub>2</sub> dissociation,<sup>86</sup> CO<sub>2</sub> reduction,<sup>87</sup> NH<sub>3</sub> synthesis,<sup>88</sup> among others.<sup>16,89</sup> But it should be emphasized that the SPs excited carriers are quite different from those of semiconductors or dyes, with regards to their energy distribution and the lifetimes, among other features (Figure 2).

### **Heat mediated thermal-chemical reaction**

Temperature can greatly change the rate of chemical reactions, often following the Arrhenius law (Figure 4e), thus one can control the yield of a chemical reaction by exploiting the heat produced following the decay of SPs.<sup>90,91</sup> Plasmonic nanostructures were first employed in 2007 as nanosources of heat to improve the chemical reaction rate.<sup>92</sup> As solar energy is one of the most promising renewable energy sources to replace fossil-based energy sources, such a reaction would have the following advantages. (1) Reducing demand for other energy sources through the heating effect of SPs. Specifically, plasmonic nanostructures can convert incident light into heat more efficiently than most other means. (2) Improving the heating dynamics through the confinement effect of SPs (Figure 5c1). Recent studies report that plasmonic nanostructures can confine the hot region to improve the heating efficiency.<sup>93-95</sup> Normally, it is difficult to localize thermal regions to the nanoscale using traditional means. This makes the plasmon-mediated heating unique and promising.

### **Factors influencing PMCR**

To efficiently power chemical reactions using SPs, one needs to understand the entire system holistically. Basically, three integral components are involved in PMCR: the SPs, the chemical reaction, and surface/interface where the reaction takes place. These three components influence PMCR; however, the various types of PMCR described above each have unique requirements relating to these three components.

1) Factors influencing SPs. SPs effects comprising the electromagnetic near-field, excited carriers, and local heating all strongly depend on size, material properties, morphology, and state of aggregation.<sup>91,96,97</sup> For instance, the SPs properties strongly depend on the geometry of the plasmonic system, by judiciously changing the geometry of the nanoparticle one can control the light harvesting ability of the

absorber to create panchromatic absorbers absorbing strongly over most of the solar spectrum.<sup>98</sup> Also the SPs properties can be greatly influenced by the space between, and the aggregation state of the plasmonic structures (Figure 1f and Figure 5c1, 5c2). For example, it was found that the photocurrent of semiconductors or dyes could be enhanced in the gap between gold nanoparticles and gold film which are also the locations of intense enhancements, so-called “hotspots”, of PEMS.<sup>99</sup> Accordingly, different types of PMCR require specific structure-designs to adjust the SPs properties to the specific applications. For example, in PEMS, the nanoparticles used range from 10 nm to 180 nm in diameter. In general, the larger size particles produce a higher enhancement of the electromagnetic field. However, the energy distribution of the excited carriers is quite different. A theoretical study teaches us that for silver nanoparticles with diameters varying from 5 nm to 25 nm, the particle size and the lifetime of the excited carriers play pivotal roles in the production rate and energy distribution. Larger nanoparticles and shorter lifetimes result in higher production rates but lower excited carrier energies.<sup>100</sup>

2) Factors influencing chemical reactions. Chemical reactions especially catalytic reactions are closely related to surface activity. In PMCR systems, three categories of mediators are usually used to improve the surface activity. (1) To fully utilize the light harvesting effect, the size of the plasmonic nanostructures, e.g. Au, Ag or Cu, should be larger than 5 nm, by contrast, in catalytic systems the larger particles often limit the catalytic activity significantly.<sup>101</sup> Thus chemical reaction mediators like Pt nanoparticles with small size are needed to compensate for the loss of catalytic-active sites (Figure 5b1). (2) The lifetime of the plasmon-induced excited carriers is too short to participate effectively in the chemical reaction (Figure 2b), leading to a low efficiency of charge transfer from the plasmonic nanostructure to the reaction precursor. Therefore, charge transfer mediators such as semiconductors are used to efficiently collect the excited carriers (Figure 4d and Figure 5b1). For instance, by using ultrafast time-resolved spectroscopy it has been shown that n-type TiO<sub>2</sub> can significantly promote the efficiency of charge separation, thus inhibiting the recombination of non-equilibrated charge carriers.<sup>102</sup> Nevertheless, this efficiency is just one aspect of the PMCR system; to date, no consensus exists on mediator selection to achieve effective charge separation. (3) The SPs-activated molecules, e.g. O<sub>2</sub> and H<sub>2</sub>, also can act as mediators. Some studies found that O<sub>2</sub> activated by accepting an excited charge carrier from the plasmonic nanostructure can enhance the catalytic oxidation reactions (Figure 5b2).<sup>103,104</sup>

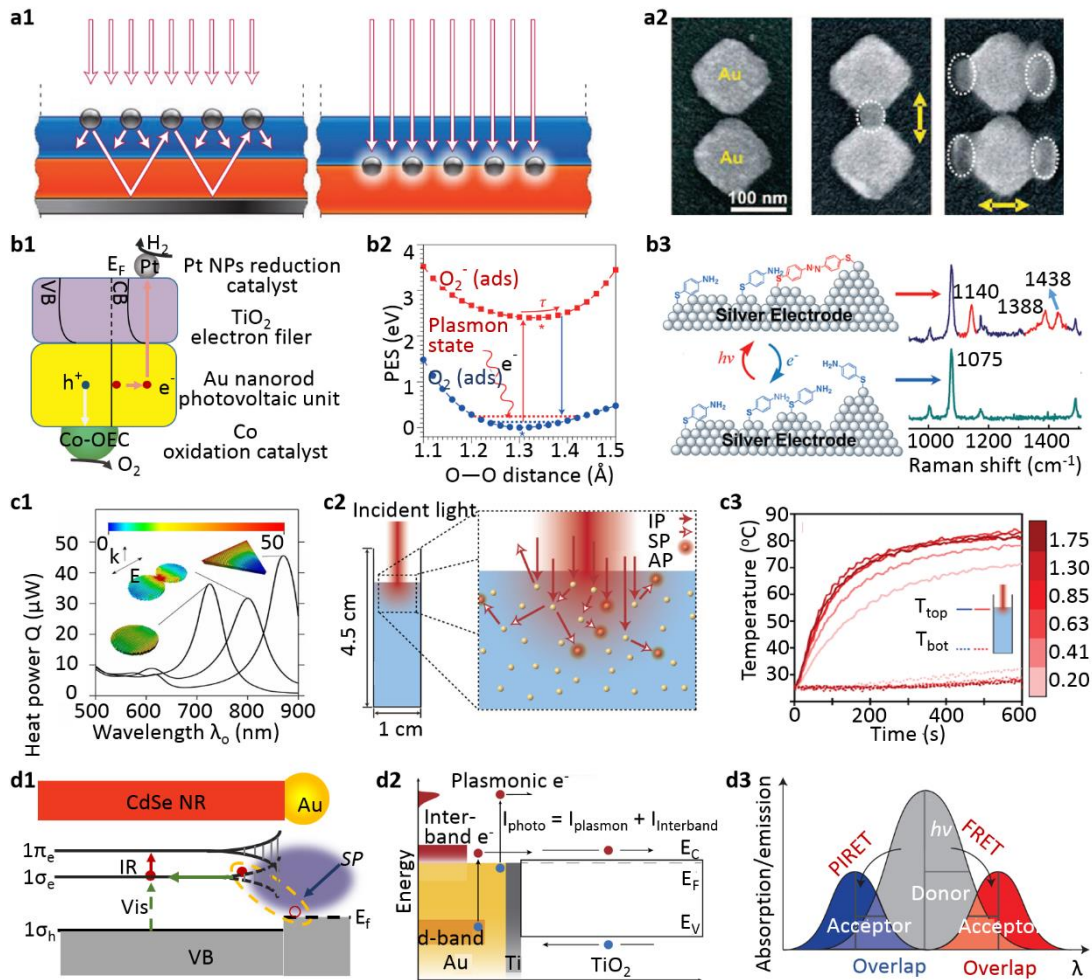


Figure 5. The three key components of PMCR: electromagnetic near-field enhancement of the photochemistry (a1-a2); SPs excited carriers to mediate the photocatalysis (b1-b3), local thermal effects promoted by SPs (c1-c3); and a graphic summary of novel mechanisms of SPs mediated energy and/or charge transfer processes (d1-d3). a1, Two basic effects of the SPs induced electromagnetic near-field enhancement: to increase the light intensity and to extend the light path, so as to increase excitation probabilities. a2, Controlling the polarized direction of the incident light, the electromagnetic near-field can induce the two-photon polymerization of SU8 in appropriate regions. b1, Schematic of a water splitting device in which the SPs induced excited carriers separate at the metal-mediator interface and participate in the redox process. Here, TiO<sub>2</sub> acts as the charge transfer mediator; Pt NPs and Co-OEC NPs act as the mediators for hydrogen evolution reaction and oxygen evolution reaction mediators, respectively; CB, VB, and E<sub>F</sub> stands for the conduction band, valence band and Fermi level, respectively. b2, Schematic depicting the O<sub>2</sub> activation, the excited electrons transfer to the absorbed oxygen to produce the transient negative ion state of O<sub>2</sub><sup>-</sup> and its subsequent relaxation can lead to vibrational energy deposition. The activated oxygen can act as the reaction mediator. b3, Scheme for the transformation from PATP to DMAB molecule induced by SPs excited electrons which can be detected, in situ, by PERS. c1, Calculated spectra of the heat generated in

nanostructures deposited on a planar glass surface immersed in water. The three insets represent the heat power density computed at the main plasmons resonance of the particle. Obviously, the local heating is related to the morphology and incident light. The color gradient indicates the heat power density ( $\text{nW}/\text{nm}^3$ ). c2, Schematic of the photo-heating in a solution of nanoparticles illuminated with 808 nm laser light. Multiparticle optical interactions by which incident photons (IP) are scattered (SP) and/or absorbed (AP) play an important role. c3, Thermal response of illuminated nanoshell solutions with different concentrations (color gradient shows the concentration as denoted, the unit is  $10^{10}$  per ml). The temperatures measured at the top and bottom of the solutions are shown as solid and dashed lines. d1, The plasmon-induced interfacial charge transfer which takes place at a metal-semiconductor interface (Au-CdSe) with strong coupling. d2, The Ohmic device (Au-Ti-TiO<sub>2</sub>) allows the carriers created by interband transition to be collected, which also contributes to the photocurrent. d3, plasmon induced resonance energy transfer (PIRET) which is different from Förster resonance energy transfer (FRET). a1, ref. 74, © 2010 NPG; a2, ref. 77, © 2008 ACS; b1, ref. 14, © 2013 NPG; b2, ref. 103, © 2011 NPG; b3, ref. 26, © 2010 ACS; c1, ref. 90, © 2009 AIP; c2, c3, ref. 95, © 2014 ACS; d1, ref. 107, © 2015 AAAS; d2, ref. 106, © 2015 NPG; d3, ref. 105, © 2015 NPG;

Furthermore, reaction processes including the adsorption and activation of the reactant, formation and retention of the intermediate, desorption of the resulting product, and the mass transport of all of the above species need also be taken into consideration in PMCR, although few studies have focused on these as yet. It is preferential to carry out chemical reactions on structurally well-defined active sites where the reaction mechanism is straightforward, and the SPs effects for the chemical reaction can be easily understood.

3) Factors influencing the contact or the surface/interface. In order to coordinate the SPs and the chemical reaction, attention should be paid to the contact or the surface/interface keeping two typical aspects in mind. (1) Mediators, especially those for the charge transfer, used to construct the heterogeneous junction for PMCR, can improve the catalytic property only when there is synergy with the plasmonic nanostructure.<sup>105</sup> One should, therefore, pay attention to the contact between the mediator and the plasmonic structure. Using the metal-semiconductor contact as an example, one can have two types of contacts: A Schottky contact and an Ohmic contact (Figure 5d2). The nature of the contact forming a heterogeneous junction (interface) can greatly influence the charge transfer process. For example, the energy barrier at the Schottky contact can be used to filter excited electrons inhibiting their recombination with the holes. The Ohmic contact, on the other hand, can permit the transfer of low-energy excited electrons, such as electrons induced by interband transitions, through the interface from the plasmonic metal to the semiconductor.<sup>106</sup> (2) Surfactants commonly used to stabilize the surface and avoid aggregation can have several impacts, including changing the plasmonic properties, and affecting the surface reaction. Additionally, SPs effects, like an enhanced electromagnetic near-field are strongly dependent on the distance from the surface. Close proximity to the

surface is usually more beneficial for catalytic reactions.

### The common ground and the differences of PEMS and PMCR

As two important branches of plasmonics, PEMS and PMCR are closely related and both are involved with three body interactions, i.e., photons, molecules and nanostructures (Figure 6a, 6b). However, PMCR (plasmon chemistry) is more complex than PEMS (plasmon physics) because in the former molecules experience transformation. Many factors such as reaction intermediates, products and yields as well as the charge transfer rates must be taken into account comprehensively (Figure 6c). This is likely the reason that the development of PMCR has lagged PEMS. It is, therefore, desirable to systematically analyze the common ground and major differences between these two branches, which is essential to meet the challenges and find the future directions of PMCR.

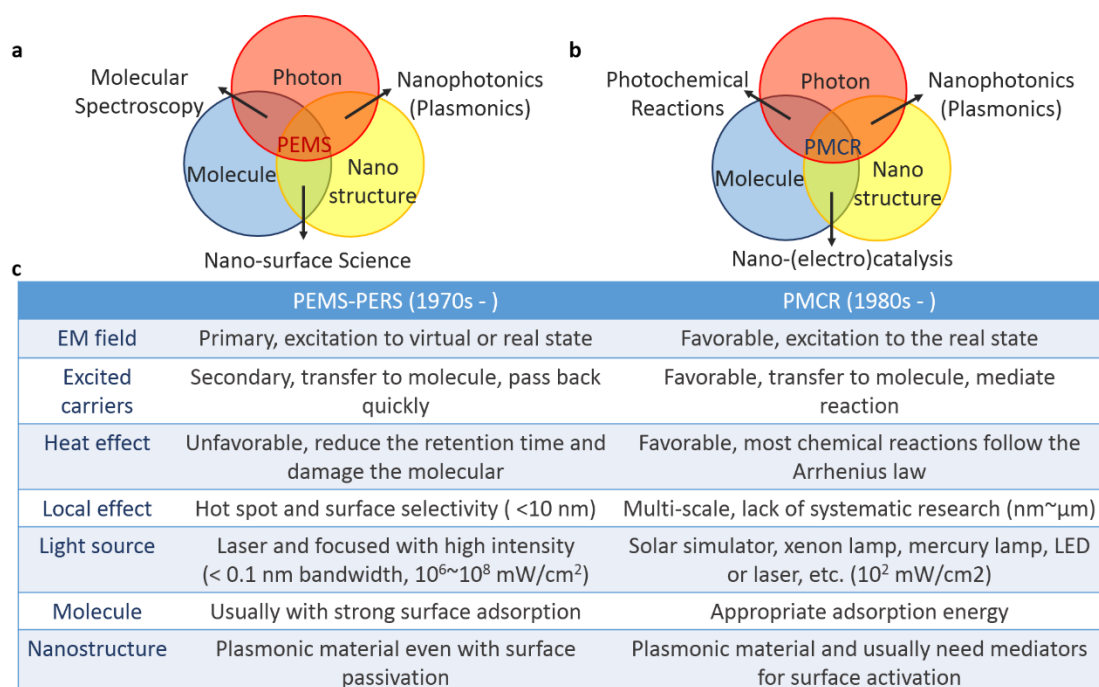


Figure 6. The comparison between PEMS and PMCR. a, The three body interaction of PEMS, including the photon, nanostructure, and molecule without chemical reaction. When only two of the three elements interact, the three separate field: nanophotonics, nano-surface science, and molecular spectroscopy arise. b, The three body interactions of PMCR, which also includes the photon, nanostructure, and molecule but with chemical reactions. c, Table comparing PEMS and PMCR with the first four rows dealing with the mechanism (electromagnetic field, excited carriers, heating effect and local effect) and the last three rows with experiment (light source, molecule and nanostructure).

PERS is the oldest member in PEMS and has been studied and applied for over four decades.<sup>5-8,11</sup> Here we use PERS as a representative to compare and differentiate PEMS and PMCR.

(1) The near-field EM enhancement. The EM mechanism is the main contribution to PERS for the enhancement of both excitation and emission. In the case of PMCR based on electromagnetic near-field, however, the emission process is absent due to the participation of excited states in chemical reactions. Moreover, the excitation of the reacting molecules or mediators in PMCR includes an electron transition from the electronic ground state to the real excited state.<sup>75,76</sup> While for PERS the electrons in the ground state are usually excited to a virtual state except in the cases of resonance or stimulated Raman scattering.<sup>11,55</sup>

(2) The SPs excited charge carriers. Charge-transfer between the plasmonic nanostructure and the reactant molecule plays a key role in PMCR.<sup>16,107</sup> Such processes may also be important in PERS when the plasmonic nanostructure forms a strong bond to the probed molecule.<sup>65</sup> They differ, however, in the final destiny of the excited carriers. In PMCR, carriers are excited and separated in order to participate in the redox chemistry which takes place at the interface of the metal and the environmental medium. In addition, the excited carriers in PMCR should have longer retention times for the reactants to take part in the reaction. Nevertheless, the excited carriers in the charge transfer process of PERS quickly decay back to the metal or the “surface complex” on a femtosecond timescale.

(3) The heating effect. Local heating is common but often ignored in plasmonic systems. For PMCR, there have been only a few systematic studies on the local heating effect, which however must clearly make a contribution to the chemical reaction, such as promoting surface desorption and mass transport. However, it is unfavorable for the detection by PERS because of the requirement of high surface-sensitivity. In addition, the Stokes and anti-Stokes Raman scattering processes are asymmetrically enhanced with a preferential increase of the anti-Stokes Raman bands in PERS.<sup>108</sup> This was first proposed to be due to the laser-induced thermal heating (“pumping”) of the ground-state molecule to the vibration-excited state.<sup>109</sup> Accordingly, the Boltzmann equation was used to calculate the local temperature rise due to the plasmon’s non-radiative decay into heat based on the PERS characteristics.<sup>110,111</sup> Many disagreements remain surrounding such calculation and what other factors are involved in the enhancement of the anti-Stokes Raman in PERS.<sup>112-114</sup> In addition, the detected PERS signals by microscope objective are usually averaged over multiple “hotspots”, the medium-enhanced and non-enhanced regions, so geometry-inhomogeneity is also a problem when using PERS to characterize the temperature. Moreover, the system becomes complex when CE and/or CT are taken into consideration. Summarizing, care must be taken when using PERS to evaluate plasmon-driven heating effects.

### **Future challenges and directions**

Despite the fact that elementary reaction mechanisms of PMCR can be explained by thermal chemistry, photo-chemistry and/or photo-catalysis, PMCR is more complex than those traditional reaction systems suggest. The probable combination of all three mechanisms especially in a nano-confined space leads to some of the unique characteristics of PMCR. The local confinement of the electromagnetic field and thermal field cause the heterogeneous distribution of the reaction area. In order to



fully take advantage of PMCR, one needs to carefully analyze the challenges and future directions according to the following five aspects.

(1) New plasmonic structures and materials. Nanostructure and composition are two critical factors controlling the spatial (position), energy (strength, wavelength), and temporal (lifetime) properties of SPs.<sup>47</sup> Nanostructures with tunable plasmonic properties would be useful in PMCR, e.g., for confining the incoming light to more localized spaces, for constructing tunable SPs with a narrow band response, for controlling the energy distribution of the excited carriers, increasing the probability of the charge transfer, and extending the lifetime of the excited carriers. Notably, a compromise between the catalytic activity and the strong optical effect is widely observed for PMCR when coinage metals are used. Some methods such as using hierarchical structures like the antenna-reactor, satellite or core-shell which are similar to the “borrowing” strategy in PEMS have been adopted.<sup>16,115-117</sup> Also, expanding the range of plasmonic materials to better accommodate PMCR is highly desirable. Some novel materials like graphene have also been shown to have SPs properties. It is important to choose suitable materials for specific applications or chemical reactions.<sup>118-120</sup> Some of these materials are usually used for catalysis. However, for these materials the plasmon resonance frequencies usually are not in the visible or near-infrared light region. Developing plasmonic materials responding at sunlight region with catalytic activity and overcoming the size gap are important goals for PMCR.

(2) Multi-scales of space, time and energy. As the electromagnetic near-field, excited carriers, and local heating are usually comingled in PMCR, to study them separately so as to determine which part is crucial for specific reactions is a useful approach. However, two barriers restrict systematic study, one is the extended time involved, spanning several femtoseconds to nanoseconds, the other is the highly localized spatial scale in nanometers.<sup>29,35-37</sup> Several strategies have been exploited to solve this problem, e.g. using insulating materials such as silica to prevent charge transfer; however, the silica coating also changes the surface, the thermal properties, etc. Silica coating even can influences the resonant energy transfer from plasmonic nanostructure to mediator or molecule.<sup>105,121</sup> Therefore, new methods, less invasive to the sample and the reaction need to be developed.

(3) Plasmon-induced excited carriers. Although plasmon-induced excited carriers have proved effective in many important reactions, the efficiencies of plasmon-mediated photocatalysis remain very low so that mediators must be applied. For example, in the case of water splitting, with the well-designed system containing charge separation mediator and reaction mediator, the highest reported external quantum efficiency is approximately 0.1% averaged over the visible portion of the solar spectrum.<sup>14</sup> Obviously, excited carriers in metals are different from those in semiconductors due to the lack of a band gap,<sup>81,82</sup> giving rise to extremely short lifetimes of the plasmon-induced excited carriers which hinder charge transfer even in the presence of mediators.<sup>32,34-39</sup> In some special cases like strong coupling, although no breakthrough has yet been reported for the overall reaction efficiency, the charge transfer efficiency can be enhanced considerably and some new charge transfer mechanisms, such as SPs induced interface charge transfer have been proposed

(Figure 4d, 5d1),<sup>107</sup> However, even for charge transfer, some key questions remain, such as how to establish the strong coupling system especially with molecules.<sup>122,123</sup> Besides, the energy distribution of the plasmon-induced excited carriers is different from that in the semiconductor and the interband transition process of the plasmonic material. More precisely, in the former case the sp-bands are supposed to be diffuse and have relatively constant density of states in the range of visible photons, which probably lead to a flat excited carrier distribution,<sup>18,39</sup> although little experimental evidence for this can be cited. Finally, the properties of hot holes are still poorly understood, with only few direct experiments reported describing their characteristics, such as their energy distribution, and lifetimes.<sup>124</sup>

(4) The localized (confinement) effect. Many materials such as semiconductors and dyes can provide excited carriers, but they are unable to confine the corresponding electric and thermal field at the nanoscale. SPs effects can not only redistribute the optical, electronic and/or thermal energy spatially at the nanoscale, but can also endow the local field with steep gradients.<sup>1,2,17,74</sup> In PMCR, the spatial distribution of the electromagnetic field, thermal field and excited carriers is non-uniform.<sup>125</sup> Logically, the localized effect of SPs should directly be able to lead to localized chemical reaction.<sup>126</sup> And it was demonstrated that SPs could controlling the chemical reactions in metal-polymer-metal gaps.<sup>127</sup> Additionally, the localized effect can influence many physical processes related to chemical reactions, such as heat transfer, mass transport, etc.<sup>94</sup> By affecting these physical processes, the SPs may influence chemical reactions in other ways. More advanced applications especially scalable ones based on the localized effect will require more than a few “hotspots” but large tracts of active surface. As with the eternal pursuit of PERS with higher sensitivity and homogeneity, expanding the ratio of the highly active sites is also crucial for PMCR.

(5) Bond-selective chemistry based on ultra-confined field of SPs. It has been proved that the tip-enhanced Raman spectroscopy is able to access the structure and conformation of a single molecule with both chemical recognition and sub-nanometer resolution.<sup>58,128</sup> The ultra-high spatial resolution is thought to result from the highly confined field and broadband nature of the nano-cavity plasmons in the tunneling gap.<sup>129</sup> This crucial breakthrough not only offers a new way to study the structural and chemical information simultaneously at the single molecule scale in PERS applications; more interestingly, it also provides a possibility to induce and manipulate chemical reactions in particular areas or groups within a single molecule under excitation of SPs, based on the fact that the local field confined by SPs can be reduced to a spot small enough to image individual groups within a single molecule, such as a methyl group or a double bond. This may result in a new, submicroscopic level of molecular processing.

## Conclusion

We have reviewed the progress in using nanostructure-based surface plasmons acting as mediators to redistribute and convert the photon energy in time, space and at various energy scales, thereby driving chemical reactions by localizing photon, electronic, and/or thermal energies. PMCR has its own scientific goals and unique characteristics distinct from existing photo- and thermal-reaction systems. For

instance, the EM field and/or the thermal field in the PMCR system are confined at the nanoscale with sharp gradients (sub-nm~nm for EM fields, and nm~ $\mu$ m for thermal fields) which can drive chemical reactions at an extreme level of spatial selectivity. In such systems, both the nano-optics and nano-thermodynamics are unique, providing opportunities through, for example, nano-confinement of mass or facile heat transfer, for novel reaction pathways with increased efficiencies or product branching possibilities. Additionally, the lifetime (< ps) and the flat energy distribution of the excited carriers in PMCR differ from what is encountered in traditional photo-catalysis (the excited carriers distribute in definite bands with ps- $\mu$ s lifetime). As a consequence, SPs can create new possibilities for powering chemical reactions.

The field of PMCR is still in an embryonic stage with two main challenges hindering its rapid development: its complex operating mechanism and its limited efficiency, especially when based on the excited carriers. PEMS has been developed over forty years and can serve as a reference for guiding the progress of PMCR. They both are molecule-specific and dependent on the three-body (molecule, incident photon and plasmonic nanostructure) interactions. To describe the mechanism of PMCR clearly, we systematically introduced various effects in time, space and energy scales. However, to improve efficiency, one needs to coordinate these effects synergistically. Significant advancements will be made, e.g., by rationally designing and fabricating plasmonic nanostructures, selecting suitable surface/interface mediators and teaming them together.

## References

1. Schuller, J. A., *et al.* Plasmonics for extreme light concentration and manipulation. *Nature Mater.* **9**, 193-204 (2010).
2. Barnes, W. L., Dereux, A. & Ebbesen, T. W. Surface plasmon subwavelength optics. *Nature* **424**, 824-830 (2003).
3. Fleischmann, M., Hendra, P. J. & McQuillan, A. J. Raman spectra of pyridine adsorbed at a silver electrode. *Chem. Phys. Lett.* **26**, 163-166 (1974).
4. Jeanmaire, D. L. & Van Duyne, R. P. Surface Raman spectroelectrochemistry: Part I. Heterocyclic, aromatic, and aliphatic amines adsorbed on the anodized silver electrode. *J. Electroanal. Chem. Interfacial Electrochem.* **84**, 1-20 (1977).
5. Moskovits, M. Surface roughness and the enhanced intensity of Raman scattering by molecules adsorbed on metals. *J. Chem. Phys.* **69**, 4159-4161 (1978).
6. Moskovits, M. Surface-enhanced spectroscopy. *Rev. Mod. Phys.* **57**, 783-826 (1985).
7. Tian, Z. Q., Ren, B. & Wu, D. Y. Surface-enhanced Raman scattering: From noble to transition metals and from rough surfaces to ordered nanostructures. *J. Phys. Chem. B* **106**, 9463-9483 (2002).
8. Ding, S. Y., You, E. M., Tian, Z. Q. & Moskovits, M. Electromagnetic theories of surface-enhanced Raman spectroscopy. *Chem. Soc. Rev.* **46**, 4042-4076 (2017).
9. Lal, S., Clare, S. E. & Halas, N. J. Nanoshell-enabled photothermal cancer therapy: Impending clinical impact. *Acc. Chem. Res.* **41**, 1842-1851 (2008).
10. Mayer, K. M. & Hafner, J. H. Localized surface plasmon resonance sensors. *Chem. Rev.* **111**, 3828-3857 (2011).

11. Stiles, P. L., Dieringer, J. A., Shah, N. C. & Van Duyne, R. P. Surface-enhanced Raman spectroscopy. *Annu. Rev. Anal. Chem.* **1**, 601-626 (2008).
12. Liebermann, T. & Knoll, W. Surface-plasmon field-enhanced fluorescence spectroscopy. *Colloids Surf., A* **171**, 115-130 (2000).
13. Emmanuel, F. & Samuel, G. Surface enhanced fluorescence. *J. Phys. D: Appl. Phys.* **41**, 013001 (2008).
14. Mubeen, S., *et al.* An autonomous photosynthetic device in which all charge carriers derive from surface plasmons. *Nature Nanotech.* **8**, 247-251 (2013).
15. Linic, S., Christopher, P. & Ingram, D. B. Plasmonic-metal nanostructures for efficient conversion of solar to chemical energy. *Nature Mater.* **10**, 911-921 (2011).
16. Clavero, C. Plasmon-induced hot-electron generation at nanoparticle/metal-oxide interfaces for photovoltaic and photocatalytic devices. *Nature Photon.* **8**, 95-103 (2014).
17. Baffou, G. & Quidant, R. Nanoplasmonics for chemistry. *Chem. Soc. Rev.* **43**, 3898-3907 (2014).
18. Christopher, P. & Moskovits, M. Hot charge carrier transmission from plasmonic nanostructures. *Annu. Rev. Phys. Chem.* **68**, 379-398 (2017).
19. Ostovar pour, S., *et al.* Through-space transfer of chiral information mediated by a plasmonic nanomaterial. *Nature Chem.* **7**, 591 (2015).
20. Nitzan, A. & Brus, L. E. Theoretical model for enhanced photochemistry on rough surfaces. *J. Chem. Phys.* **75**, 2205-2214 (1981).
21. Chen, C. J. & Osgood, R. M. Direct observation of the local-field-enhanced surface photochemical reactions. *Phys. Rev. Lett.* **50**, 1705-1708 (1983).
22. Chen, X. J., Cabello, G., Wu, D. Y. & Tian, Z. Q. Surface-enhanced Raman spectroscopy toward application in plasmonic photocatalysis on metal nanostructures. *J. Photochem. Photobiol., C* **21**, 54-80 (2014).
23. Suh, J. S., Moskovits, M. & Shakhsempour, J. Photochemical decomposition at colloid surfaces. *J. Phys. Chem.* **97**, 1678-1683 (1993).
24. Suh, J. S., Jang, N. H., Jeong, D. H. & Moskovits, M. Adsorbate photochemistry on a colloid surface: Phthalazine on silver. *J. Phys. Chem.* **100**, 805-813 (1996).
25. Brus, L. Noble metal nanocrystals: Plasmon electron transfer photochemistry and single-molecule Raman spectroscopy. *Acc. Chem. Res.* **41**, 1742-1749 (2008).
26. Huang, Y. F., *et al.* When the signal is not from the original molecule to be detected: Chemical transformation of para-Aminothiophenol on Ag during the SERS measurement. *J. Am. Chem. Soc.* **132**, 9244-9246 (2010).
27. Wimmer, E., Fu, C. L. & Freeman, A. J. Catalytic promotion and poisoning: All-electron Local-density-functional theory of CO on Ni(001) surfaces coadsorbed with K or S. *Phys. Rev. Lett.* **55**, 2618-2621 (1985).
28. Alayoglu, S., Nilekar, A. U., Mavrikakis, M. & Eichhorn, B. Ru-Pt core-shell nanoparticles for preferential oxidation of carbon monoxide in hydrogen. *Nature Mater.* **7**, 333-338 (2008).
29. Ozbay, E. Plasmonics: Merging photonics and electronics at nanoscale dimensions. *Science* **311**, 189-193 (2006).
30. Maier, S. A., *et al.* Local detection of electromagnetic energy transport below the diffraction limit in metal nanoparticle plasmon waveguides. *Nature Mater.* **2**, 229-232 (2003).
31. Le Ru, E. C. & Etchegoin, P. G. Chapter 3 - Introduction to plasmons and plasmonics. in *Principles of Surface-Enhanced Raman Spectroscopy* 121-183 (Elsevier, Amsterdam, 2009).

32. Link, S. & El-Sayed, M. A. Spectral properties and relaxation dynamics of surface plasmon electronic oscillations in gold and silver nanodots and nanorods. *J. Phys. Chem. B* **103**, 8410-8426 (1999).
33. Hao, F., *et al.* Symmetry breaking in plasmonic nanocavities: Subradiant LSPR sensing and a tunable Fano resonance. *Nano Lett.* **8**, 3983-3988 (2008).
34. Frischkorn, C. & Wolf, M. Femtochemistry at metal surfaces: Nonadiabatic reaction dynamics. *Chem. Rev.* **106**, 4207-4233 (2006).
35. Khurgin, J. B. How to deal with the loss in plasmonics and metamaterials. *Nature Nanotech.* **10**, 2-6 (2015).
36. Cho, G. C., Dekorsy, T., Bakker, H. J., Hövel, R. & Kurz, H. Generation and relaxation of coherent majority plasmons. *Phys. Rev. Lett.* **77**, 4062-4065 (1996).
37. Inouye, H., Tanaka, K., Tanahashi, I. & Hirao, K. Ultrafast dynamics of nonequilibrium electrons in a gold nanoparticle system. *Phys. Rev. B* **57**, 11334-11340 (1998).
38. Bonn, M., *et al.* Phonon- versus electron-mediated desorption and oxidation of CO on Ru(0001). *Science* **285**, 1042-1045 (1999).
39. Brongersma, M. L., Halas, N. J. & Nordlander, P. Plasmon-induced hot carrier science and technology. *Nature Nanotech.* **10**, 25-34 (2015).
40. Osawa, M., Ataka, K. I., Yoshii, K. & Nishikawa, Y. Surface-enhanced infrared spectroscopy: The origin of the absorption enhancement and band selection rule in the infrared spectra of molecules adsorbed on fine metal particles. *Appl. Spectrosc.* **47**, 1497-1502 (1993).
41. Aroca, R. F., Ross, D. J. & Domingo, C. Surface-enhanced infrared spectroscopy. *Appl. Spectrosc.* **58**, 324A-338A (2004).
42. Ortolani, M. & Limaj, O. Surface-enhanced infrared spectroscopy. in *Handbook of Enhanced Spectroscopy* 443-483 (Pan Stanford, 2015).
43. Tian, Z. Q., Ren, B., Li, J. F. & Yang, Z. L. Expanding generality of surface-enhanced Raman spectroscopy with borrowing SERS activity strategy. *Chem. Commun.* **34**, 3514-3534 (2007).
44. Stadler, J., Schmid, T. & Zenobi, R. Developments in and practical guidelines for tip-enhanced Raman spectroscopy. *Nanoscale* **4**, 1856-1870 (2012).
45. Li, J. F., Anema, J. R., Wandlowski, T. & Tian, Z. Q. Dielectric shell isolated and graphene shell isolated nanoparticle enhanced Raman spectroscopies and their applications. *Chem. Soc. Rev.* **44**, 8399-8409 (2015).
46. Gruenke, N. L., *et al.* Ultrafast and nonlinear surface-enhanced Raman spectroscopy. *Chem. Soc. Rev.* **45**, 2263-2290 (2016).
47. Ding, S. Y., *et al.* Nanostructure-based plasmon-enhanced Raman spectroscopy for surface analysis of materials. *Nat. Rev. Mater.* **1**, 16021 (2016).
48. Li, J. F., Li, C. Y. & Aroca, R. F. Plasmon-enhanced fluorescence spectroscopy. *Chem. Soc. Rev.* **46**, 3962-3979 (2017).
49. Gray, S. K. Surface plasmon-enhanced spectroscopy and photochemistry. *Plasmonics* **2**, 143-146 (2007).
50. Le Ru, E. C. & Etchegoin, P. G. Chapter 4 - SERS enhancement factors and related topics. in *Principles of Surface-Enhanced Raman Spectroscopy* 185-264 (Elsevier, Amsterdam, 2009).
51. Etchegoin, P. G. & Le Ru, E. C. Basic electromagnetic theory of SERS. in *Surface Enhanced Raman Spectroscopy* 1-37 (Wiley-VCH Verlag GmbH & Co. KGaA, 2010).
52. Ding, S. Y., Zhang, X. M., Ren, B. & Tian, Z. Q. Surface-enhanced Raman spectroscopy (SERS):

- general introduction. in *Encyclopedia of Analytical Chemistry* (John Wiley & Sons, Ltd, 2006).
53. Wang, X., *et al.* Tip-enhanced Raman spectroscopy for surfaces and interfaces. *Chem. Soc. Rev.* **46**, 4020-4041 (2017).
  54. Schmid, T., Opilik, L., Blum, C. & Zenobi, R. Nanoscale chemical imaging using tip-enhanced Raman spectroscopy: A critical review. *Angew. Chem. Int. Ed.* **52**, 5940-5954 (2013).
  55. Schlücker, S. Surface-enhanced Raman spectroscopy: Concepts and chemical applications. *Angew. Chem. Int. Ed.* **53**, 4756-4795 (2014).
  56. Michaels, A. M., Nirmal, M. & Brus, L. E. Surface enhanced Raman spectroscopy of individual Rhodamine 6G molecules on large Ag nanocrystals. *J. Am. Chem. Soc.* **121**, 9932-9939 (1999).
  57. Nie, S. & Emory, S. R. Probing single molecules and single nanoparticles by surface-enhanced Raman scattering. *Science* **275**, 1102-1106 (1997).
  58. Zhang, R., *et al.* Chemical mapping of a single molecule by plasmon-enhanced Raman scattering. *Nature* **498**, 82-86 (2013).
  59. Yampolsky, S., *et al.* Seeing a single molecule vibrate through time-resolved coherent anti-Stokes Raman scattering. *Nature Photon.* **8**, 650-656 (2014).
  60. Kerker, M., Wang, D. S. & Chew, H. Surface enhanced Raman scattering (SERS) by molecules adsorbed at spherical particles. *Appl. Opt.* **19**, 3373-3388 (1980).
  61. Gersten, J. & Nitzan, A. Electromagnetic theory of enhanced Raman scattering by molecules adsorbed on rough surfaces. *J. Chem. Phys.* **73**, 3023-3037 (1980).
  62. Aravind, P. K., Nitzan, A. & Metiu, H. The interaction between electromagnetic resonances and its role in spectroscopic studies of molecules adsorbed on colloidal particles or metal spheres. *Surf. Sci.* **110**, 189-204 (1981).
  63. Otto, A. *Surface-enhanced Raman scattering: "Classical" and "Chemical" origins* (Springer Berlin Heidelberg, 1984).
  64. Tian, Z. Q. General Discussion. *Faraday Discuss.* **132**, 147-158 (2006).
  65. Wu, D. Y., Li, J. F., Ren, B. & Tian, Z. Q. Electrochemical surface-enhanced Raman spectroscopy of nanostructures. *Chem. Soc. Rev.* **37**, 1025-1041 (2008).
  66. Schatz, G. C. & Van Duyne, R. P. Electromagnetic mechanism of surface-enhanced spectroscopy. in *Handbook of Vibrational Spectroscopy* (John Wiley & Sons, Ltd, 2006).
  67. Petek, H. Photoexcitation of adsorbates on metal surfaces: One-step or three-step. *J. Chem. Phys.* **137**, 091704 (2012).
  68. Klessinger, M. & Michl, J. *Excited States and Photochemistry of Organic Molecules* (VCH Publishers, New York, 1995).
  69. Turro, N. J. *Modern Molecular Photochemistry* (University Science Books, Mill Valley, CA, 1991).
  70. Karny, Z. & Zare, R. N. Infrared laser photochemistry: Evidence for heterogeneous decomposition. *Chem. Phys.* **23**, 321-325 (1977).
  71. Zare, R. N. Laser Control of Chemical Reactions. *Science* **279**, 1875-1879 (1998).
  72. Ottosson, H. Exciting excited-state aromaticity. *Nature Chem.* **4**, 969 (2012).
  73. Van Leeuwen, T., Lubbe, A. S., Štacko, P., Wezenberg, S. J. & Feringa, B. L. Dynamic control of function by light-driven molecular motors. *Nat. Rev. Chem.* **1**, 0096 (2017).
  74. Atwater, H. A. & Polman, A. Plasmonics for improved photovoltaic devices. *Nature Mater.* **9**, 205-213 (2010).
  75. Liu, Z., Hou, W., Pavaskar, P., Aykol, M. & Cronin, S. B. Plasmon resonant enhancement of photocatalytic water splitting under visible illumination. *Nano Lett.* **11**, 1111-1116 (2011).

76. Ingram, D. B. & Linic, S. Water splitting on composite plasmonic-metal/semiconductor photoelectrodes: Evidence for selective plasmon-induced formation of charge carriers near the semiconductor surface. *J. Am. Chem. Soc.* **133**, 5202-5205 (2011).
77. Ueno, K., *et al.* Nanoparticle plasmon-assisted two-photon polymerization induced by incoherent excitation source. *J. Am. Chem. Soc.* **130**, 6928-6929 (2008).
78. Murdoch, M., *et al.* The effect of gold loading and particle size on photocatalytic hydrogen production from ethanol over Au/TiO<sub>2</sub> nanoparticles. *Nature Chem.* **3**, 489 (2011).
79. Roger, I., Shipman, M. A. & Symes, M. D. Earth-abundant catalysts for electrochemical and photoelectrochemical water splitting. *Nat. Rev. Chem.* **1**, 0003 (2017).
80. Honda, K. & Fujishima, A. Electrochemical photolysis of water at a semiconductor electrode. *Nature* **238**, 37-38 (1972).
81. Linsebigler, A. L., Lu, G. & Yates, J. T. Photocatalysis on TiO<sub>2</sub> surfaces: Principles, mechanisms, and selected results. *Chem. Rev.* **95**, 735-758 (1995).
82. Wang, Q., *et al.* Scalable water splitting on particulate photocatalyst sheets with a solar-to-hydrogen energy conversion efficiency exceeding 1%. *Nature Mater.* **15**, 611-615 (2016).
83. Denzler, D. N., Frischkorn, C., Hess, C., Wolf, M. & Ertl, G. Electronic excitation and dynamic promotion of a surface reaction. *Phys. Rev. Lett.* **91**, 226102 (2003).
84. Tian, Y. & Tatsuma, T. Plasmon-induced photoelectrochemistry at metal nanoparticles supported on nanoporous TiO<sub>2</sub>. *Chem. Commun.* 1810-1811 (2004).
85. Mukherjee, S., *et al.* Hot-electron-induced dissociation of H<sub>2</sub> on gold nanoparticles supported on SiO<sub>2</sub>. *J. Am. Chem. Soc.* **136**, 64-67 (2014).
86. Martirez, J. M. P. & Carter, E. A. Excited-state N<sub>2</sub> dissociation pathway on Fe-functionalized Au. *J. Am. Chem. Soc.* **139**, 4390-4398 (2017).
87. Hou, W., *et al.* Photocatalytic conversion of CO<sub>2</sub> to hydrocarbon fuels via plasmon-enhanced absorption and metallic interband transitions. *ACS Catal.* **1**, 929-936 (2011).
88. Oshikiri, T., Ueno, K. & Misawa, H. Plasmon-induced ammonia synthesis through nitrogen photofixation with visible light irradiation. *Angew. Chem. Int. Ed.* **53**, 9802-9805 (2014).
89. Zhang, N., *et al.* Near-field dielectric scattering promotes optical absorption by platinum nanoparticles. *Nature Photon.* **10**, 473-482 (2016).
90. Baffou, G., Quidant, R. & Girard, C. Heat generation in plasmonic nanostructures: Influence of morphology. *Appl. Phys. Lett.* **94**, 153109 (2009).
91. Baffou, G. & Quidant, R. Thermo-plasmonics: using metallic nanostructures as nano-sources of heat. *Laser Photonics Rev.* **7**, 171-187 (2013).
92. Cao, L., Barsic, D. N., Guichard, A. R. & Brongersma, M. L. Plasmon-assisted local temperature control to pattern individual semiconductor nanowires and carbon nanotubes. *Nano Lett.* **7**, 3523-3527 (2007).
93. Yang, Q., Xu, Q., Yu, S. H. & Jiang, H. L. Pd Nanocubes@ZIF-8: Integration of plasmon-driven photothermal conversion with a metal-organic framework for efficient and selective catalysis. *Angew. Chem. Int. Ed.* **55**, 3685-3689 (2016).
94. Kim, K., *et al.* Radiative heat transfer in the extreme near field. *Nature* **528**, 387-391 (2015).
95. Hogan, N. J., *et al.* Nanoparticles heat through light localization. *Nano Lett.* **14**, 4640-4645 (2014).
96. Govorov, A. O., Zhang, H., Demir, H. V. & Gun'ko, Y. K. Photogeneration of hot plasmonic electrons with metal nanocrystals: Quantum description and potential applications. *Nano*

- Today* **9**, 85-101 (2014).
97. Sundararaman, R., Narang, P., Jermyn, A. S., Goddard, W. A. III & Atwater, H. A. Theoretical predictions for hot-carrier generation from surface plasmon decay. *Nature Commun.* **5**, 5788 (2014).
  98. Mubeen, S., Lee, J., Liu, D., Stucky, G. D. & Moskovits, M. Panchromatic photoproduction of H<sub>2</sub> with surface plasmons. *Nano Lett.* **15**, 2132-2136 (2015).
  99. Harutyunyan, H., *et al.* Anomalous ultrafast dynamics of hot plasmonic electrons in nanostructures with hot spots. *Nature Nanotech.* **10**, 770-774 (2015).
  100. Manjavacas, A., Liu, J. G., Kulkarni, V. & Nordlander, P. Plasmon-induced hot carriers in metallic nanoparticles. *ACS Nano* **8**, 7630-7638 (2014).
  101. Haruta, M. Size- and support-dependency in the catalysis of gold. *Catal. Today* **36**, 153-166 (1997).
  102. Furube, A., Du, L., Hara, K., Katoh, R. & Tachiya, M. Ultrafast plasmon-induced electron transfer from gold nanodots into TiO<sub>2</sub> nanoparticles. *J. Am. Chem. Soc.* **129**, 14852-14853 (2007).
  103. Christopher, P., Xin, H. & Linic, S. Visible-light-enhanced catalytic oxidation reactions on plasmonic silver nanostructures. *Nature Chem.* **3**, 467-472 (2011).
  104. Huang, Y. F., *et al.* Activation of oxygen on gold and silver nanoparticles assisted by surface plasmon resonances. *Angew. Chem. Int. Ed.* **53**, 2353-2357 (2014).
  105. Li, J., *et al.* Plasmon-induced resonance energy transfer for solar energy conversion. *Nature Photon.* **9**, 601-607 (2015).
  106. Zheng, B. Y., *et al.* Distinguishing between plasmon-induced and photoexcited carriers in a device geometry. *Nature Commun.* 7797 (2015).
  107. Wu, K., Chen, J., McBride, J. R. & Lian, T. Efficient hot-electron transfer by a plasmon-induced interfacial charge-transfer transition. *Science* **349**, 632-635 (2015).
  108. Maher, R. C., *et al.* Stokes/anti-Stokes anomalies under surface enhanced Raman scattering conditions. *J. Chem. Phys.* **120**, 11746-11753 (2004).
  109. Sushchinskii, M. M. & Rousseau, D. L. Raman spectra of molecules and crystals. *Phys. Today* **26**, 61-62 (2008).
  110. Sun, M., Zhang, Z., Zheng, H. & Xu, H. In-situ plasmon-driven chemical reactions revealed by high vacuum tip-enhanced Raman spectroscopy. *Sci. Rep.* **2**, 647-650 (2012).
  111. Zhang, Z., *et al.* Insights into the nature of plasmon-driven catalytic reactions revealed by HV-TERS. *Nanoscale* **5**, 3249-3252 (2013).
  112. Haslett, T. L., Tay, L. & Moskovits, M. Can surface-enhanced Raman scattering serve as a channel for strong optical pumping? *J. Chem. Phys.* **113**, 1641-1646 (2000).
  113. Brolo, A. G., Sanderson, A. C. & Smith, A. P. Ratio of the surface-enhanced anti-Stokes scattering to the surface-enhanced Stokes-Raman scattering for molecules adsorbed on a silver electrode. *Phys. Rev. B* **69**, 045424 (2004).
  114. Maher, R. C., *et al.* Resonance contributions to anti-Stokes/Stokes ratios under surface enhanced Raman scattering conditions. *J. Chem. Phys.* **123**, 084702 (2005).
  115. Li, J. F., *et al.* Shell-isolated nanoparticle-enhanced Raman spectroscopy. *Nature* **464**, 392-395 (2010).
  116. Robotjazi, H., *et al.* Plasmon-induced selective carbon dioxide conversion on earth-abundant aluminum-cuprous oxide antenna-reactor nanoparticles. *Nature Commun.* **8**, 27 (2017).
  117. Aslam, U., Chavez, S. & Linic, S. Controlling energy flow in multimetallic nanostructures for



- plasmonic catalysis. *Nature Nanotech.* **12**, 1000-1005 (2017).
118. Grigorenko, A. N., Polini, M. & Novoselov, K. S. Graphene plasmonics. *Nature Photon.* **6**, 749-758 (2012).
  119. Lalisse, A., Tessier, G., Plain, J. & Baffou, G. Quantifying the efficiency of plasmonic materials for near-field enhancement and photothermal conversion. *J. Phys. Chem. C* **119**, 25518-25528 (2015).
  120. Voiry, D., Shin, H. S., Loh, K. P. & Chhowalla, M. Low-dimensional catalysts for hydrogen evolution and CO<sub>2</sub> reduction. *Nat. Rev. Chem.* **2**, 0105 (2018).
  121. Cushing, S. K., *et al.* Photocatalytic Activity Enhanced by Plasmonic Resonant Energy Transfer from Metal to Semiconductor. *J. Am. Chem. Soc.* **134**, 15033-15041 (2012).
  122. Chikkaraddy, R., *et al.* Single-molecule strong coupling at room temperature in plasmonic nanocavities. *Nature* **535**, 127-130 (2016).
  123. Benz, F., *et al.* Single-molecule optomechanics in "picocavities". *Science* **354**, 726-729 (2016).
  124. Schlather, A. E., *et al.* Hot Hole Photoelectrochemistry on Au@SiO<sub>2</sub>@Au Nanoparticles. *J. Phys. Chem. Lett.* **8**, 2060-2067 (2017).
  125. Zhu, W., *et al.* Quantum mechanical effects in plasmonic structures with subnanometre gaps. *Nature Commun.* **7**, 11495 (2016).
  126. Cortés, E., *et al.* Plasmonic hot electron transport drives nano-localized chemistry. *Nature Commun.* **8**, 14880 (2017).
  127. Wang, P., Krasavin, A. V., Nasir, M. E., Dickson, W. & Zayats, A. V. Reactive tunnel junctions in electrically driven plasmonic nanorod metamaterials. *Nature Nanotech.* **13**, 159-164 (2018).
  128. Zhang, Y., *et al.* Visualizing coherent intermolecular dipole-dipole coupling in real space. *Nature* **531**, 623-627 (2016).
  129. Zhang, Y., *et al.* Sub-nanometre control of the coherent interaction between a single molecule and a plasmonic nanocavity. *Nature Commun.* **8**, 15225 (2017).

### **Acknowledgements**

We are deeply grateful to M. Moskovits for his very helpful suggestions and careful academic and English editing throughout the manuscript. This work is financially supported by the National Natural Science Foundation of China (21533006, 21621091, 91427304 and 21403180) and the Ministry of Science and Technology of China (2015CB932300).

### **Author contributions**

Z-Q.T conceived the outline. C.Z., X-J.C and Z-Q.T. wrote the manuscript. J.Y. supplied the calculation in the Figure1. All authors contributed to discussions, editing and corrections. C.Z. and Z-Q.T. revised the manuscript before the final submission.

### **Competing interests statement**

The authors declare no competing financial interests.